41. *Aftershocks that accompanied the Tottori Earthquake of Sept. 10, 1943. (The 2nd Paper)*

By Syun'itiro OMOTE,

Earthquake Research Institute.

(Read Sept. 16, 1953.—Received Sept. 30, 1955.)

1. Introduction

On the evening of Sept. 10, 1943, the Tottori area was shaken by a severe earthquake. This area is near the coast of the Japan Sea in the western part of the Island of Honshu. The magnitude of this earthquake was estimated as 7.4 by the Gutenberg Richter scale. It resulted in the destruction of more than 7000 dwelling houses and the loss of more than 1000 human lives. Tottori is the largest city in the damaged area and the earthquake is named after it. Prior to this Tottori earthquake, this same area was shaken by two somewhat slighter shocks on March 4 and 5 of the same year which resulted only in the destruction of five houses[1]. After these shocks a somewhat large number of afterschocks, about 537 times in all, were felt in the same area before the destructive earthquake broken out on Sept. 10. The Tottori earthquake was highly destructive in the epicentral area and was the biggest one to occur in these parts along the coast of the Japan Sea after the great Tango earthquake of March 3, 1944, that was originated 80 km to the east of this earthquake.

In less than 24 hours after the outbreak of the Tottori earthquake a field party of our Institute was organized and dispatched to the shaken area, the writer being held responsible for the observation of aftershocks. After a seismometer was installed at Igumi (Fig. 1) on the Sept. 12, seismic stations were established one after another and by the evening of Sept. 14 eight stations, each having one component of horizontal pendulum, were in operation.

The observation of aftershocks was continued for about a month and the description of the distribution of seismic foci of some selected aftershocks was given in a preliminary report published in 1944[2]. As

1) S. OMOTE, *Bull. Earthq. Res. Inst.*, **21** (1943), 453.
2) S. OMOTE, *Bull. Earthq. Res. Inst.*, **22** (1944), 33.

this map of foci was prepared in a great hurry on the basis of rough calculations made immediately after the main shock took place, it was necessary to prepare a more complete report. However, as the war became gradually severe the analysis of the seismograms had to be put aside for many years till recently when all the seismograms were thoroughly readjusted in order to locate the more reliable foci of aftershocks. The results of the readjustment are reported here.

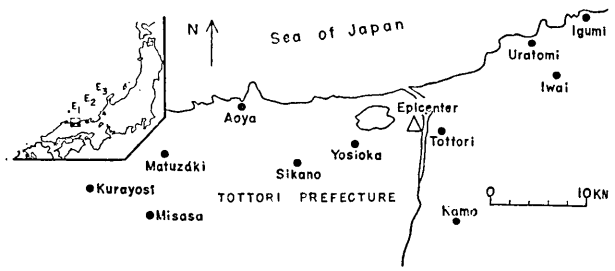

Fig. 1. Map of Tottori district, showing locations of the epicenter of the main shock and the observation network of the aftershocks.

- ● observation point
- △ epicenter of the main shock
- ▲ E_1, Tottori Earthq.: E_2, Tango Earthq.: E_3, Fukui Earthq.

2. General sketch of the activity of the Tottori aftershocks

From the data of the station observatories, the epicenter was located by the Central Meteolorogical Observatory[3] at 134.°2 E longitude, 35.5° N latitude. The observation network for the aftershocks was placed at the beginning over the eastern part of the Prefecture, but later a seismic fault was found on Sept. 16 near Sikano Town, 15 km to the south-west of Tottori, and on Sept. 28, a fairly large shock of intensity IV according to the Japanese Intensity Scale broke out near Kurayosi Town, and the network had to be shifted gradually to the west.

In this observation of the Tottori aftershocks, as was the case with the other earthquakes, the driving power of the recording drum of the seismograph was fed by an AC motor. The electric power supply, however, was shut off owing to the disconnection of power cables at many places caused by the severe earthquake vibrations. Owing to the wartime situation, the repair works of the damaged power cables went on very slowly, especially in the hilly regions of the southern part of the Prefecture. From this reason we encountered some restrictions in distributing the observation points.

Locations of the observation points, the types of the seismographs

3) *Seismological Bulletin of the CMO*, Japan, for the year 1943.

installed and their instrumental constants and the length of the period of observations are tabulated in Table I. In order to set up as many observation stations as possible, we were compelled to do with only one seismometer at each station, as there were only eight seismometers in all that were available for us.

Table I. Instrumental constants of the seismometers installed at the temporary observation points and the length of the period of observation.

Observation point	Component	Observed Period from month	date	to month	date	Weight of the mass of pendulum	Free oscillation period	Magnification
Uradomi	H-1	IX	16	IX	18	7.5kg	0.12sec	ca. 100
Iwai	〃	IX	27	X	8	6	6.0	21
Igumi	〃	IX	12	IX	23	7.5	0.12	100
Tottori	〃	IX	13	IX	23	7.5	0.12	100
	〃	IX	23	X	12	13	0.15	213
Kamo	〃	IX	13	IX	20	7.5	0.12	100
Yosioka	〃	IX	15	X	11	6	6.0	21
Makihara	〃	IX	21	X	5	7.5	0.12	100
Sikano	〃	IX	14	X	9	7.5	0.12	100
Aoya	〃	IX	18	X	9	7.5	0.12	100
Kurayosi	〃	IX	16	IX	24	6	6.0	21
	〃	IX	24	X	10	7.5	0.12	100
Matuzaki	〃	X	7	X	11	7.5	0.12	100
Misasa	〃	X	8	X	10	7.5	0.12	100

3. Number of aftershocks

On the third day after the great earthquake the first seismograph of our field party was installed in the shaken area but it took two more days before the network of our observation of aftershocks could be completely established and began its operations in full. The Tottori Branch Station of the CMO counted the number of aftershocks (of course only the sensible ones) and the hourly number of the aftershocks felt is reproduced in Fig. 2 by the courtesy of CMO[4]. This figure attracts our attentions especially in the point the hourly number of aftershocks is seen increasing for the first few hours after the occurrence of the

4) W. INOUYE, *Report of the Tottori Earthquake of Sept. 10 1943*, *CMO*, (1943), (in Japanese).

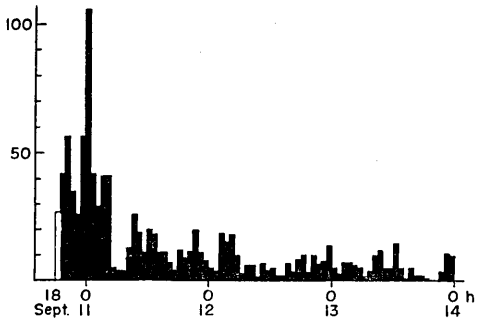

Fig. 2. Hourly number of aftershocks felt at Tottori Branch Station of CMO.

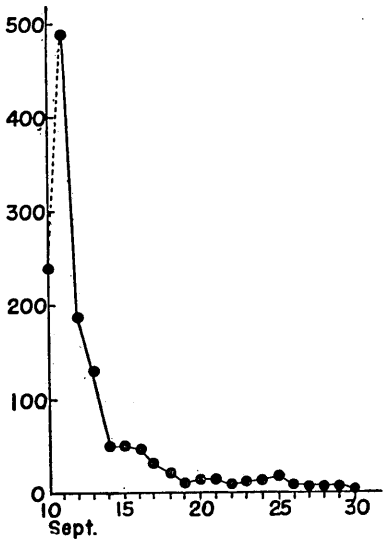

Fig. 3. Daily number of felt aftershocks at the Tottori Branch Station of CMO.

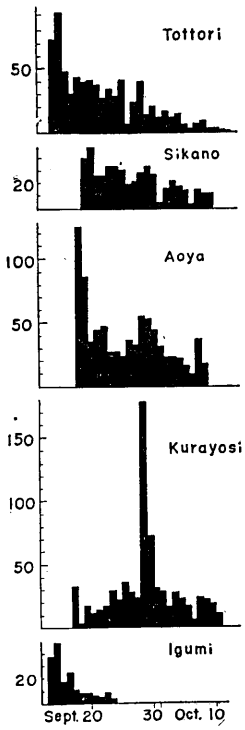

Fig. 4. Daily number of aftershocks.

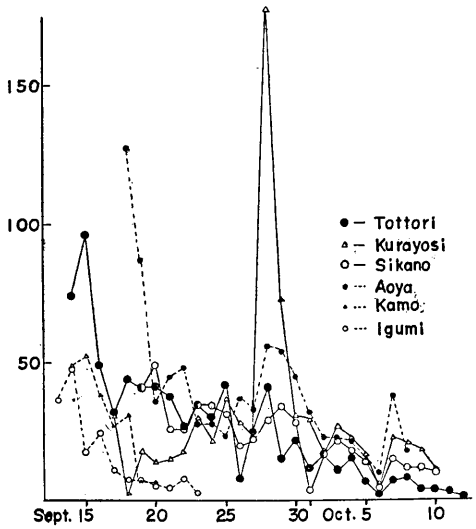

Fig. 5. Daily number of aftershocks at Tottori, Sikano, Kurayosi, Igumi, Kamo and Aoya.

main shock. Six hours after the main shock the hourly number of aftershocks reached its maximum and then it began to decrease rapidly with the lapse of time. The daily number of aftershocks is seen in Fig. 3. The figure shows that the generation of aftershocks was very active for two or three days after the main shock but after Sept. 14 the activity became less vivid. From this it will be seen that, though our observation net was installed in a great hurry, the most active and important period for the study of the aftershocks escaped our observations. The daily number of aftershocks recorded at each station of our seismograph network is given in Fig. 4.

For the purpose of showing the general tendency of the seismic activity throughout the entire shaken area, the daily number of the aftershocks at different stations is shown together in one sheet (Fig. 5). From this figure it is seen that such stations as Igumi, Kamo and Tottori, that are situated in the eastern area were active in the early period of our investigation, while they became inactive as time went on compared with the activity of the western stations. The most noticeable activity is seen in the curves of Kurayosi Station. In this station the number of shocks was rather few compared with that of the Tottori Station until Sept. 28, but after that date, on which date a strong shock took place near the Kurayosi Station, the number of shocks observed at the Kurayosi Station is seen to exceed the number of any other station.

4. Frequency distribution of P-S time

Fig. 6 shows the frequency diagrams of P-S time at respective stations. We notice in the first place that the maximum frequency of P-S time appears to be at about 1 second at the respective stations. On further examination, however, it is found that at Tottori Station the most frequently occurring P-S time is 0.6–1.0 sec., and at Sikano and Kurayosi Stations 0.9–1.0 sec., while at Aoya and Kamo it becomes somewhat longer, being 1.5 sec. or so. In the second place we notice that a very short P-S time is observed at almost every station, especially in Tottori Station, where such a short P-S time as only 0.2–0.4 sec. is observed for about 20 times. If we assume, for instance, that the P–S time is 0.2 sec., it turns out that the distance between the station and the hypocenter is only 1.6 km or so. This means that we have to expect that the earthquake occurs in such a shallow point even if it took place right under the observation station. In general these earthquakes with very short P-S time are also small in their amplitudes and from this

fact we are inclined to think that quite a number of very small shocks were taking place over a wide area covering the whole disturbed area. With respect to the Aoya Station no such shock with very short P-S time was to be seen taking place. In the third place, we notice that in this case of the Tottori aftershocks, fairly long P-S times were also observed at some stations, though they were small in number. At the Sikano Station, which is situated in the central part of our observation network, shocks with P-S time longer than 5 seconds were not recorded at all. At the Tottori and Igumi Stations situated in the eastern part of our observation network, or at the Kurayosi and Aoya Stations situated at the western end of our network, the P-S time exceeding 7 or 8 seconds could be observed though small in number. These facts may give some indication as to the geographical distribution of the foci of the aftershocks.

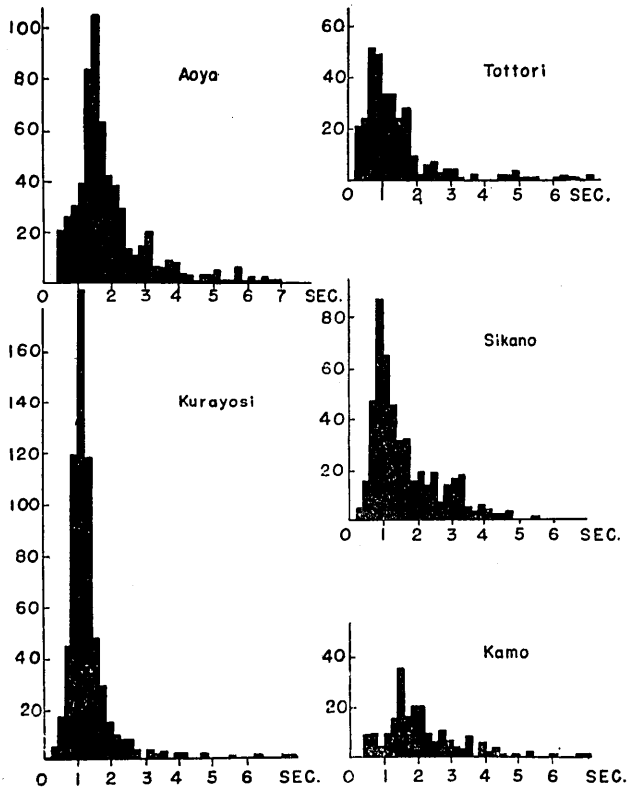

Fig. 6. Frequency diagram of P-S time.

A word should be added as to the P-S time of the Kurayosi Station. In Fig. 7 the frequency diagram of P-S time observed at the Kurayosi Station is shown, in which (b) is in the period from Sept. 16 to Sept. 27 and (a) from Sep. 28 to Oct. 10. As we have already seen, on Sept. 28 a fairly large shock took place near the Kurayosi station and subsequently the seismicity of this station became suddenly active from that date, so that it was considered that there may be seen some differences in the form of frequency diagrams between the two periods. As will

be shown in Figs. 7-a and b, in which (b) is a P–S diagram in the former period and (a) in the latter period, shocks of the shorter P–S time appear to be somewhat active in the latter period.

5. Determination of epicenters

The P–S interval method was introduced in determining the foci of shocks. In this method the value of k, the constant factor in the formula $D=kt$[5], has been determined graphically through those earthquakes that have given good records at least four stations. Those shocks which were used for the determination of k are tabulated in Table II with the value of k

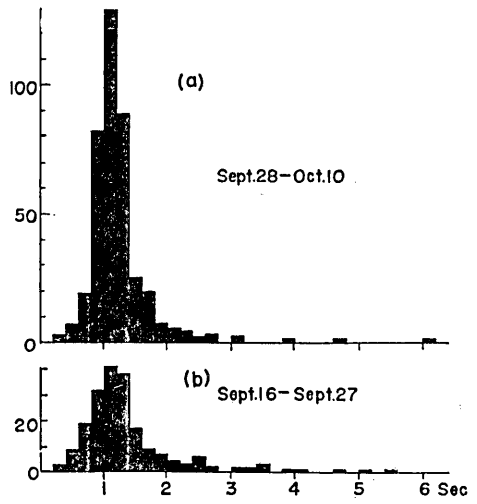

Fig. 7. Frequency diagram of P-S time at Kurayosi Station.

Table II. List of aftershocks for the determination of k. P–S time, value of k and H, the depth of focus.

Earthq. No.	Time of occurrence	Tottori	Yosi-oka	Maki-hara	Sika-no	Aoya	Matu-zaki	Kura-yosi	Misasa	k	H
	Sept. h m	sec.	sec.	sec.							km
1*	15 0 25	1.0	1.0							7.4	4.8
7	21 14 32	1.6	1.4	1.4	1.7					8.3	10.8
11	24 3 25	1.8	1.3	1.8	1.1	2.4				7.0	9.3
13	24 13 20	4.2		2.9	2.7			1.9		9.0	11.4
14	27 01 33	2.7		1.7	1.3			2.3		8.6	10.3
17	28 06 41	4.3		2.8	2.4	2.4		1.2		8.1	5.0
	Oct.										
28	3 02 10			3.2	2.7	2.1		1.8		8.8	13.1
29	3 02 11			3.7	3.0	2.6		2.2		9.0	18.8
32	7 5 30					1.9	1.0	1.2	0.8	8.0	6.4
36	7 22 11				2.6	2.1	0.9	0.9	0.9	7.1	4.6
38	9 5 28					1.6	1.1	1.5	1.2	8.1	8.2
									mean	8.1±0.45	

* Igumi, 3.1 sec; Kamo, 1.9 sec.

5) F. OMORI, *Rep. Imp. Earthq. Inv. Comm.*, (*in Japanese*), **88 A** (1918), 1.

as well as their P–S times. The mean value of k is obtained as 8.1 ± 0.4.

The numerical value of k is found to be much smaller in the usual case of other aftershocks, as is shown in Table III. It is seen from the table that the value of k ranges from 4 to 6 which is smaller than the value of k obtained by Omori through the earthquakes that were generated in the Kwanto District. In the usual case of the observation

Table III. Constant factor k obtained at different earthquakes.

Date			Earthquake	k
1927	III	17	Tango Earthquake[6]	8.41
1930	III	—	Ito Earthquake Swarm[7]	4.70
1930	IX	26	North Idu Earthquake[8]	5.13 ± 0.29
1935	IV	21	Formosa Earthquake[9]	4.79
1936	II	21	Koti-Yamato Earthquake[10]	6.15
1938	VI	—	Ooshima Swarm[11]	2.2+0.4d
1939	V	1	Ogasima Earthquake[12]	5.1 ± 0.3
1940	XII	12	Miyake-sima Eruption[13]	(2)
1943	IX	10	Tottori Earthquake	8.1 ± 0.41
1944	XII	7	Tōkaido Earthquake[14]	7.1+0.02d
1945	I	13	Mikawa Earthquake[15]	5.7
1948	VI	28	Fukui Earthquake[16]	7.2
1949	XII	26	Imaichi Earthquake[17]	7.1 ± 0.4

of aftershocks, even the largest epicentral distance does not exceed 40 or 50 km, so that it is considered that the P–S times may be derived from the waves $\overline{P}(\overline{S})$ or P*(S*). These facts, together with the shallow depth of their foci, may be responsible for the small value of k. Com-

6) N. NASU, *Jour. Facul. Sci. Imp. Univ. Tokyo*, II, **3** (1929), 29.
7) N. NASU, F. KISHINOUYE and T. KODAIRA, *Bull. Earthq. Res. Inst.*, **9** (1931), 32.
8) N. NASU, *Bull. Earthq. Res. Inst.*, **13** (1935), 400.
9) N. NASU, *Bull. Earthq. Res. Inst., Suppl. Vol.*, **3** (1936), 75.
10) N. NASU and T. HAGIWARA, *Bull. Earthq. Res. Inst.*, **14** (1936), 285.
11) R. TAKAHASI, *do.* **16** (1938), 87.
12) T. HAGIWARA *do.* **18** (1940) 252.
13) T. HAGIWARA, *do.* **19** (1941) 260.
14) T. MINAKAMI and S. UTIBORI, *do.* **24** (1946), 19.
15) S. OMOTE, *do.* **24** (1946), 77.
16) S. OMOTE, *et. al. Report of the Fukui Earthq.*, (1949), 37.
17) EARTHQ. RES. INST., *Bull. Earthq. Res. Inst.*, **28** (1951), 387.

pared with these small values of k, the Tottori earthquake is noticeable for its large value of k. A large value of k is also seen in the case of the Tango earthquake in 1927 and the Fukui earthquake in 1948. The Tottori area is very near the Tango district (Fig. 1) and these areas, existing in the northern part of Western Honsyu, are widely covered by granitic rocks.[18] The main reason for the large value of k obtained at the Tottori and Tango earthquakes may be attributed to the geological structures of the districts.

Making use of this value of k, it was possible to determine the epicenters of such shocks of which the P–S times were observed at only three stations. In the case of the Tottori aftershocks, as was the case with the other ones, large number of very small shocks were seen occurring very near a station, while they could not be recorded at distant stations. Moreover, in the case of Tottori aftershocks it was especially difficult to find correspondence between seismograms obtained at different stations, because the supply of the electric AC commercial current was interrupted from time to time, stopping in turn the revolution of a recording drum several times a day. Shocks of which the correspondence was not so reliable were rejected from our calculation and only those shocks of which correspondence was good were used in the determination of epicenters. There are 100 shocks of which the epicenters were determined. Geographical distribution of the epicenters is shown in Fig. 8. Epicenters were found to be distributed in the area 40 km long and 20 km wide with Tottori City situated in the eastern border and Kurayosi Town in the western border of the seismically active area. Such distribution of seismic foci of aftershocks as seen in Fig. 8, may of course have something to do with the distribution of the observation net itself, but nevertheless it will be safe to say that this map shows the seismic active area of the Tottori aftershocks.

In the case of the Tottori earthquake, two seismic faults, Sikano and Yosioka faults, were formed. With respect to these faults, a detailed description is given by Tsuya[19] and their locations are reproduced after him in the map of foci of aftershocks (Fig. 8). We note that almost all the foci of aftershocks are generated in the northern area of the fault, although nothing can be said for a small number of foci that are located on the other side of the fault. We find from this figure that the seismic activity is to be seen mainly in the area bounded by

18) H. Tsuya, *Bull. Earthq. Res. Inst.*, **4** (1928), 139.
19) H. Tsuya, *Bull. Earthq. Res. Inst.*, **22** (1944), 1.

two lines, the line of the coast of the Japan Sea to the north, and the fault line that ties Tottori and Sikano to the south. In the period from the beginning of our observation (Sept. 14), to Sept. 28 seismic

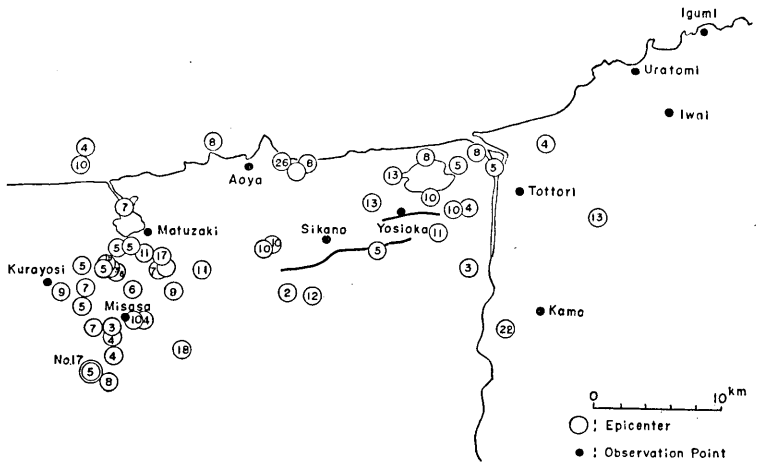

Fig. 8. Distribution of seismic foci.

foci are seen densely distributed in the eastern part of the area described above, while from Sept. 28 to Oct. 5 they are much more densely distributed in the western part of the area.

6. Cubic distribution of the foci

In Fig. 8 the numerals in the circles indicating the epicenters represent the depth of the focus in kilometers. The frequency distribution of the depth of focus is shown in Fig. 9. As shown by the numerals the focal depths of some shocks are very small, while those of some others are as deep as 25 km, but, in most cases, the depth is about 10 km. For the purpose of making clear the cubic distribution of the aftershocks the seismic foci that are distributed in the area bounded by the fault line in the south and the coastal line of the Japan Sea in the north are projected to the vertical plane intersecting the surface along the line of the Sikano fault (line B–B' in Fig. 10-a). As in Fig. 10-b, somewhat deep shocks are generated in the central area while shallow shocks are generated in the east and west parts. In Figs. 10-c and 10-d are shown the cubic distribution of foci that are projected

to the verical plane intersecting the surface along the lines AA' and CC' with respect to the aftershocks that are generated in the areas A and C (Fig. 10-a), respectively. As to the Tottori area (Fig. 10-c)

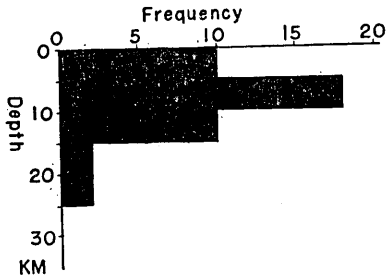

Fig. 9. Frequency diagram of focal depth.

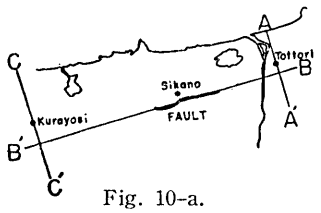

Fig. 10-a.

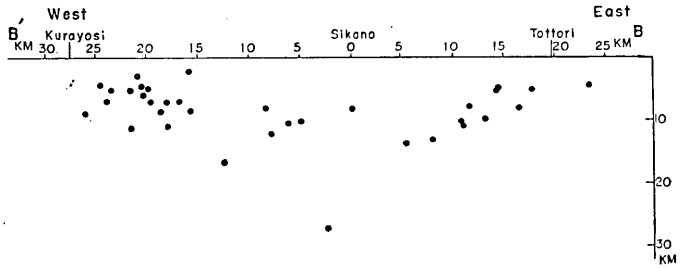

Fig. 10-b. Cubic distribution of seismic foci projected to the vertical plane BB' that runs parallel to the fault line.

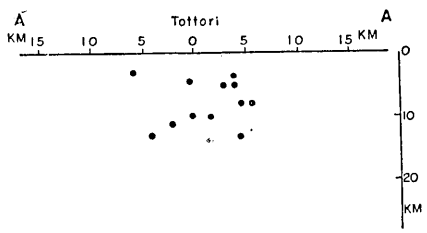

Fig. 10-c. Cubic distribution of seismic foci projected to the vertical plane AA' that is perpendicular to the fault line.

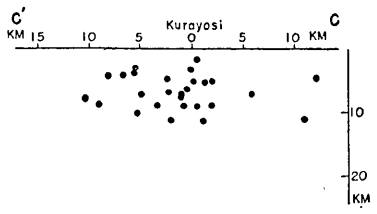

Fig. 10-d. Cubic distribution of seismic foci projected to the vertical plane CC' that is perpendicular to the fault line.

deeper foci is seen in the southern part and in the Kurayosi area (Fig. 10-d) shocks of the very shallow origin are seen to have taken place.

7. Frequency distribution of maximum amplitude

Ishimoto and Iida[20] have proposed an empirical formula on the frequency distribution of maximum amplitudes of earthquakes observed at Tokyo of the form:

$$N(a)=ka^m \tag{1}$$

where a is the maximum amplitude of a shock, $N(a)$ the number of shocks of which the maximum amplitude is between a and $a+da$, k and m being numerical constants. Asada and Suzuki[21] have shown that this relation holds good for much smaller earthquakes than those treated

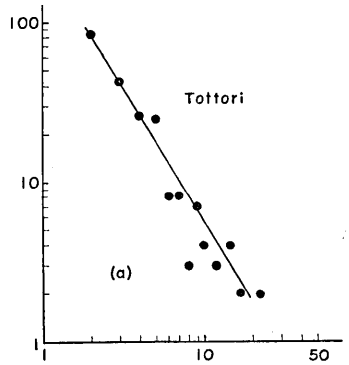

Fig. 11 (a)

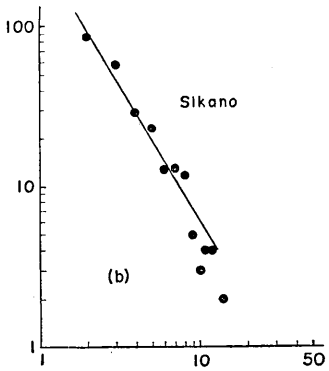

Fig. 11 (c)

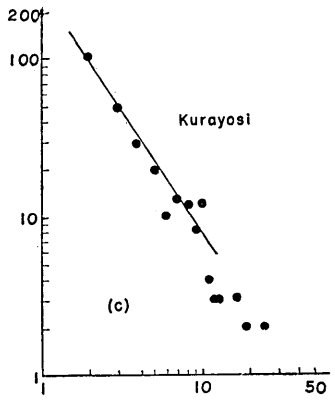

Fig. 11 (b)

Fig. 11. Frequency distribution of maximum amplitudes at different stations.
a; Tottori Station, b; Sikano Station, c; Kurayosi Station.

20) M. ISHIMOTO and K. IIDA, *Bull. Earthq. Res. Inst.*, **17** (1939), 443.
21) T. ASADA and Z. SUZUKI, *Geophys. Notes*, **2** (1949), No. 2.

by Ishimoto and Iida. The frequency of maximum trace amplitudes of earthquake as a function of amplitude observed at three stations, Tottori, Sikano and Kurayosi are shown in Fig. 11.

The values of m in equation (1) calculated from these figures are

Tottori	$m=-1.82\pm0.16$
Sikano	$m=-1.88\pm0.12$
Kurayosi	$m=-1.79\pm0.07$

These values of m are very near to those obtained in the case of other aftershocks such as Fukui[22] and Imaichi[23].

8. Magnitudes of observed aftershocks

Many authorities have proposed methods of determining the magnitude of an earthquake from the trace amplitudes observed at seismic stations. We made some study of finding out the magnitude of aftershocks recorded at our temporary stations. In our observations the distribution of seismic net was limited to the area in Fig. 1, so that there was no means of knowing the amplitude or intensities of shocks at its epicentral distance at 100 km. Tsuboi[24] has proposed a formula which can conveniently be used for determining the Richter-Gutenberg's instrumental magnitude M of an earthquake from the observation at any epicentral distance. The proposed formula is

$$M=0.20\Delta+0.67\log A+3.80\,, \qquad \Delta<5 \tag{2}$$

where Δ is the epicentral distance measured in 100 km and A the maximum vibration amplitude of the ground measured in micron. After the present paper was read, Tsuboi[25] revised his formula as follows:

$$M=1.73\log\Delta+\log A-0.83$$

the reason being that the coefficient of log A will be more reasonably taken as unity. But as asserted in the paper referred to the main object of calculating the magnitude of an earthquake is to estimate approximately the intensity of the earthquake, so for convenience' sake the values of the magnitude M of each aftershock, which has been calculated by using the former formula were adopted in this paper without modi-

22) T. ASADA, *Report of the Fukui Earthq.*, (1949), 58.
23) T. ASADA and Z. SUZUKI, *Bull. Earthq. Res. Inst.*, **28** (1950), 415.
24) C. TSUBOI, *Geophysical Notes*, **4** (1951), No. 5.
25) C. TSUBOI, *Zisin* (*Jour. Seis. Soc. Japan*) [ii], **7** (1954), 185.

fying them by using the latter formula.

In the course of the calculation of the magnitude from equation (2), it becomes necessary to know the epicentral distance and the maximum displacement amplitude of the ground. An epicentral distance will easily be known from the P–S time multiplied by $k(=8.1)$, while the amplitude of the ground displacement is not so easy to know. As we have already seen in Table I, the free oscillation period of our seismometers are about 0.1 sec. while the period of a large amplitude of a ground wave ranged from 0.2 to 0.6 sec. Accordingly it may be said that the seismometer records the acceleration of the earth movement.

Theoretically speaking, it is possible to have a computed displacement seismogram from a accelerogram observed[26], provided one does not shrink from the labour of calculation, and from such a computed displacement seismogram the true maximum amplitude will easily be obtained. But considering the accuracy and the nature of the problem of determining the magnitude of an earthquake, such a troublesome calculation is not worth while at all. As may be seen in the plates the maximum acceleration is given by the waves in the beginning part of S phase, while according to our experience the maximum amplitude of the displacement seismogram of a near shock is also seen in the waves in the beginning part of S phase[27]. Such being the case, it is probably not so misleading if we assume the result calculated from the maximum trace acceleration amplitude to be the maximum displacement amplitude. From this standpoint we assumed that the maximum displacement amplitude Ae is given by

$$Ae=\frac{1}{V}\cdot\frac{T^2}{4\pi^2}\alpha_e$$

where α_e is the maximum trace acceleration amplitude, T the period of that acceleration, and V the magnification constant of that instrument. Moreover, there lies another difficulty in calculating the true maximum displacement amplitude of the ground, because in the case of our observation, only one seismometer was installed at each station. In the calculation of the magnitude, the maximum amplitude A is defined as the one which is the square root of the sum of the squares of the component maximum amplitudes Ae, the east-west component, and An, the north-south component, and the fact that Ae and An are not necessarily

26) T. HAGIWARA, *Bull. Earthq. Res. Inst.*, **13** (1935), 138.
27) T. ASADA, *Zisin* (*Jour. Scis. Soc. Japan*) [ii], **6** (1953), 69.

the two components of one and the same vibration is ignored. Only one component is available from our stations, so that assuming that $Ae=An$ (this assumption seems not to be a too unreasonable one judging from the reports of seismometrical observations)[28], the maximum displacement amplitude A was taken as $A=\sqrt{2}Ae$. Through such procedures as described above, since Δ and A are known for each shock observed at the respective stations, the magnitude M of each shock is easily determined from the formula (2).

Table IV. Magnitude M determined at different stations.

Earthq. No.	Time of occurrence	Tottori	Maki-hara	Sikano	Aoya	Matu-zaki	Kura-yosi	Misasa	Mean of M
	Sept. h m								
7	21 14 32	3.6	3.7	3.5					3.58±0.08
10	23 21 58	3.4	3.5	3.9					3.58±0.20
11	24 3 25	3.5	3.5	3.6	3.6				3.53±0.06
13	24 13 20	3.3	3.3	3.4			3.4		3.36±0.04
14	27 01 33	3.5	3.3	3.4			3.5		3.38±0.09
15	27 12 17	3.1	3.9	3.3			3.1		3.33±0.24
17	28 6 41	4.2	4.3	4.5			4.3		4.13±0.12
	Oct.								
25	2 01 50	2.5		2.7	2.1		2.7		2.49±0.20
26	2 18 46	3.5		3.2	3.1		3.4		3.28±0.12
27	2 02 07	3.6		3.5	3.4		3.0		3.38±0.16
28	3 02 10	3.6	3.4	3.6	3.6		4.0		3.64±0.16
29	3 02 11	2.5	2.6	2.9	2.5		2.4		2.57±0.12
30	4 01 11			2.7	2.5		2.4		2.53±0.01
32	7 05 30			3.0	3.2		2.6	3.2	3.00±0.14
33	7 09 05				3.3		3.8	3.5	3.50±0.17
34	7 11 01	4.2		4.0	4.1		4.1		4.11±0.04
36	7 22 11			3.2	3.1	3.2	3.0	3.8	3.27±0.20
38	8 03 37				2.7	2.6	2.4	3.0	2.66±0.16
39	8			3.0	3.2	2.9	3.0	2.9	2.99±0.01
41	9 05 28					2.3	2.1	2.3	2.20±0.08
42	10					2.4	2.3	2.2	2.30±0.06

With respect to these aftershocks of which the foci have been determined from the observations at four stations (Table II), the magnitudes were also calculated on the basis of each record obtained at the four respective stations and the result is shown in Table IV. As will be

28) For instance, *CMO, The Seismological Bulletin of CMO, Japan.*

seen in the table the diversity in the value of M is not so large and the probable deviation δM is given in the last column of the table. The shocks listed in this table are rather large ones which accompanied the Tottori earthquake. With these rather large shocks it is seen from the table that the magnitude M ranges from 4 to 5.

From these values of M the energy will be calculated through the formula[29]

$$\log E = 12 + 1.8\, M\,.$$

M and E were calculated with respect to all the aftershocks recorded at four stations, Tottori, Sikano, Aoya and Kurayosi.

For the purpose of studying the seismic activity in the area covered by the observation net as a whole, we divided the whole area into three semispheres that have their centers at Tottori, Sikano and Kurayosi respectively, and the radii of which are 9.7 km, 10.5 km and 15.4 km respectively (Fig. 12). This means that in the first semisphere all the shocks observed at the Tottori station with the P–S time less than 1.2 sec. are included in it, and in the second and the third semisphere, likewise, all the shocks recorded at Sikano and Kurayosi with P–S time under 1.3 sec. and 1.9 sec. respectively, are included in the respective semisphere.

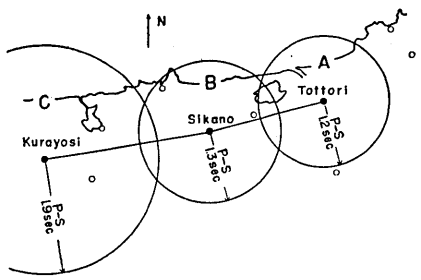

Fig. 12.

As we know from Table I, there are very few shocks that have a focal depth less than 6 km, so that it will be safe to say that the shocks that are recorded at three stations, Tottori Sikano and Kurayosi, and having the P–S time less than 1.2, 1.3, and 1.9 sec. respectively are included in any one of these three semispheres without repetition. Now we will call these semispheres A, B and C in order from east to west.

In order to know some measure on the amount of the energy released from the aftershocks that have taken place in the respective areas A, B and C, the square root of the energy E calculated from the shocks observed at stations Tottori, Sikano and Kurayosi were summed up with time respectively and is shown in Fig. 13-a, b, c where each circular dot represents an increment of energy from a single shock. We see from this figure that the sum of energies released increases step-wise by

29) B. GUTENBERG and C.F. RICHTER, *Bull. Seis. Soc. Amer.*, **32** (1942), 163.

every relatively large shock.

Seismic energies sent out from the areas A, B and C respectively every two days are shown by three curves in Fig. 14, from which

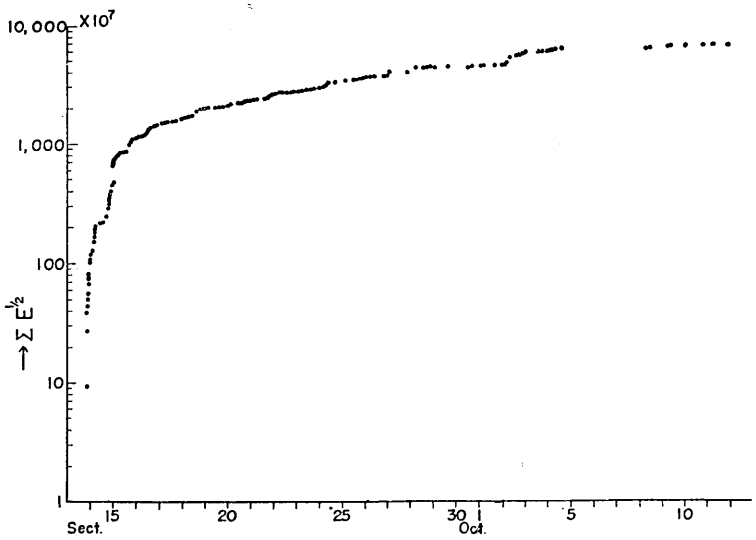

Fig. 13–a. Strain increment in the A area.

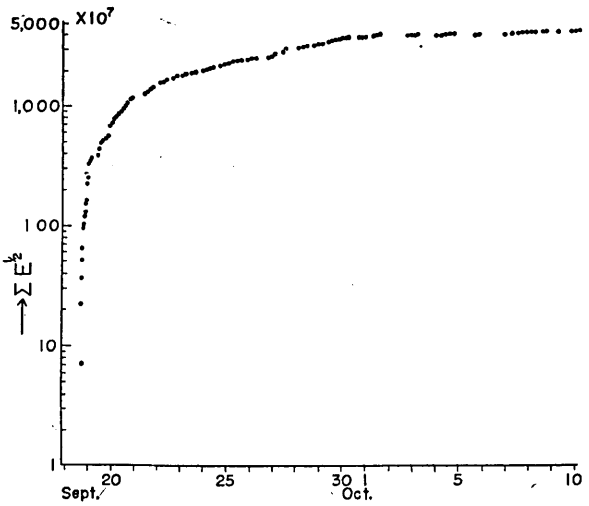

Fig. 13–b. Strain increment in the B area.

seismic activities in the respective areas will clearly be seen. In the A area, namely the Tottori area, seismic activity is found to be moderately

high through the entire period observed, while in the *C* area seismic activity is found to be somewhat low in the first half of the period, while after Sept. 28 the seismicity becomes more active than the two

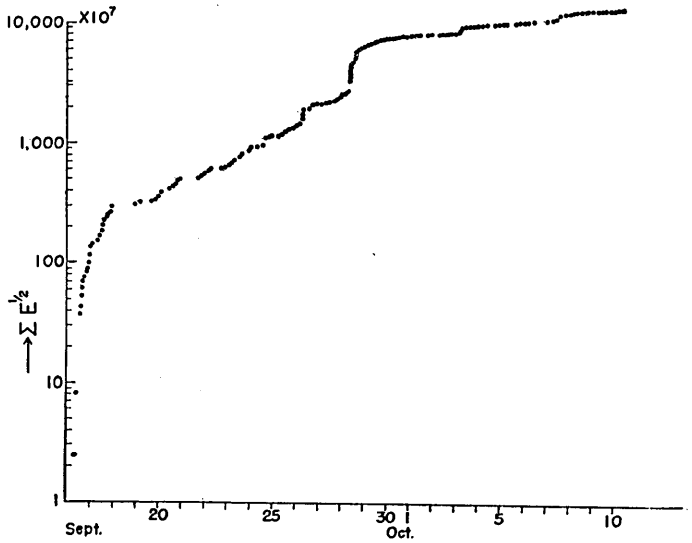

Fig. 13-c. Strain increment in the C area.

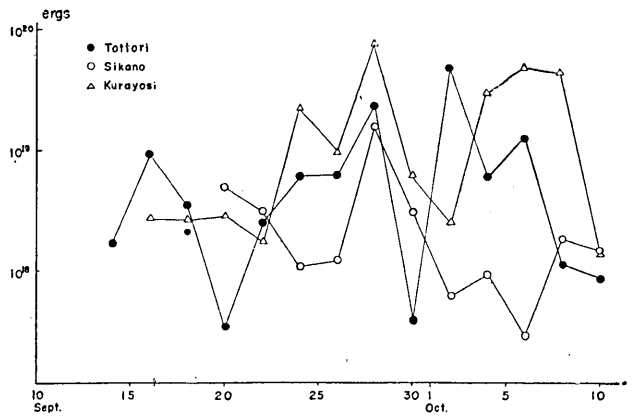

Fig. 14. Seismic energies send out from the respective areas *A*, *B* and *C*, every two days.

other areas. With respect to the *B* area (Sikano area) it is found that the activity is the lowest compared with the former two areas.

9. Frequency distribution of the magnitude of aftershocks

Since the statistical studies of energy and frequency of earthquake were first made by Gutenberg and Richter[30] in 1944, many authorities have developed the study in this direction. Gutenberg and Richter proposed a formula in the form

$$\log N = a + b(8 - M)$$

where N is the number of earthquake of which the magnitude M is $M-0.25 < M < M+0.25$. For the shocks which occurred in South California and having the value of M between 4 and 6 they obtained the numerical value of the constant b as $b=0.88\pm0.03$. Tsuboi[31] got the value of b as $b=1.04$ by making use of earthquakes that have occurred in and near Japan in the periods from 1931 to 1950. On the other hand Kawasumi[32] obtained a relation between N and M_K, the magnitude scale defined by himself, of the form $N(M_K)=\text{const}\times 10^{-0.56M_K}$, and after that Asada has studied the frequency distribution of the magnitude M_K through the minor earthquakes that occurred in the Kwanto District. In his case M_K was between 4 to 1. He got the relation

$$\log N(M_K) = \text{const} - 0.58\, M_K.$$

In the case of Tottori aftershocks frequencies of the magnitude M of shocks in the respective areas A, B and C, are shown in the semilog paper in Fig. 15. By the least square method values of the constant b are given as

A	area (Tottori area)	$b=0.95\pm0.05$
B	area (Sikano area)	$b=1.09\pm0.06$
C	area (Kurayosi area)	$b=0.88\pm0.04$

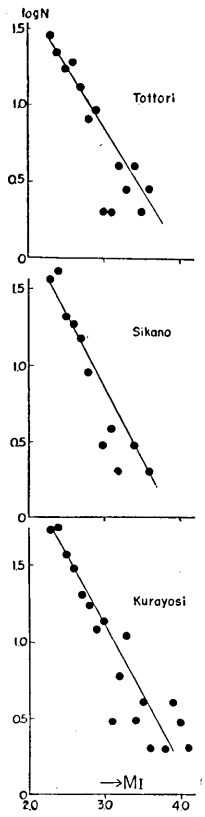

Fig. 15. Frequency diagram of equal interval of magnitude M.

10. Frequency distribution of the energy of aftershocks

Instead of classifying the earthquake by the equal intervals of magnitude M, let us now consider the number of earthquakes classified

30) B. GUTENBERG and C. F. RICHTER, *Bull. Seis. Soc. Amer.*, **34** (1944), 185.
31) C. TSUBOI, *Jour. Physics of the Earth*, **1** (1952), 47.
32) H. KAWASUMI, *Bull. Earthq. Res. Inst.*, **30** (1952), 185.

by the equal interval of energy E.

Asada[33] and others have derived an equation

$$N(E)E\,dE=\text{const}\times E^{-0.5}dE \tag{3}$$

where $N(E)$ is the number of earthquakes of which the energy is between E and $E+dE$. We transfer the equation (3) in the form

$$\log N=\text{const}-(1+\alpha)\log E,$$

and from the data here obtained, the value of constant α will be determined as

in the area B $\quad\alpha=0.54\pm0.12$

in the area C $\quad\alpha=0.54\pm0.14$

with respect to all the shocks originated in the whole areas, A, B and C, we get the relation between $\log N$ and $\log E$ as will be seen in Fig. 14 and from it we obtain the value of constant α as $\alpha=0.55\pm0.15$. This value is a little larger compared with the theoretical value, but anyhow this result shows that, as Asada and others already pointed out, according to the classification of equal interval of energy, the total energy released in the class E and $E+dE$ becomes smaller with the increase in E.

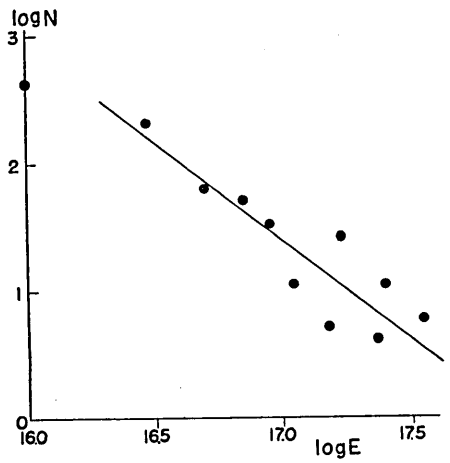

Fig. 16. Frequency diagram of equal interval of E.

As we have already seen in paragraph 7, the Ishimoto Iida's formula was applied satisfactorily in this case of Tottori earthquake, so that it is quite natural that we should have come to this conclusion concerning the frequency of energies of aftershocks. And this in turn may indicate that the magnitude scale here adopted is usefull in the determination of the magnitude of such small earthquake as aftershocks.

In conclusion the author wishes to express his hearty thanks to

33) T. ASADA, Z. SUZUKI and Y. TOMODA, *Bull. Earthq. Res. Inst.*, **29**, (1951), 289.

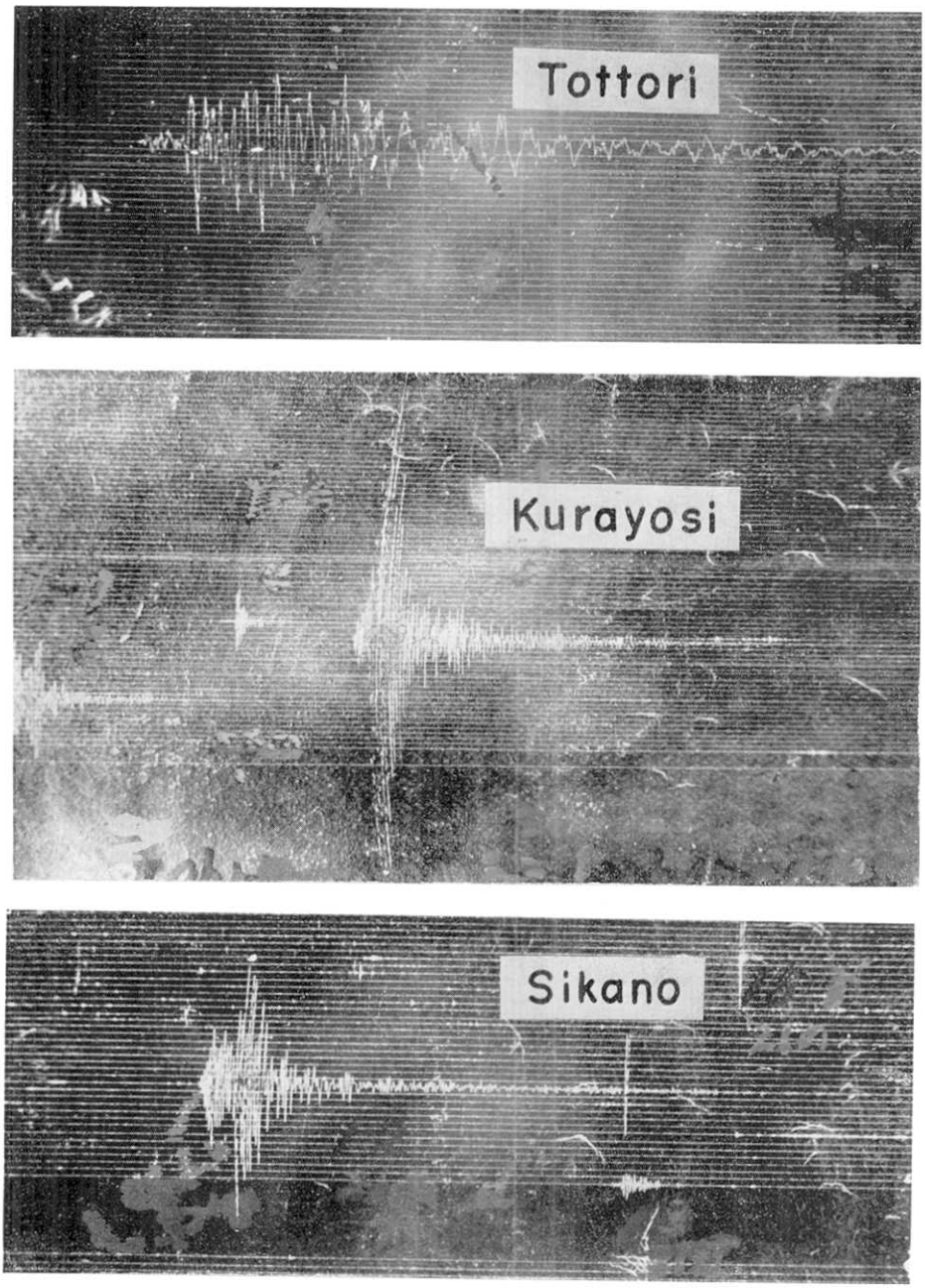

Seismograms of the Tottori aftershocks.

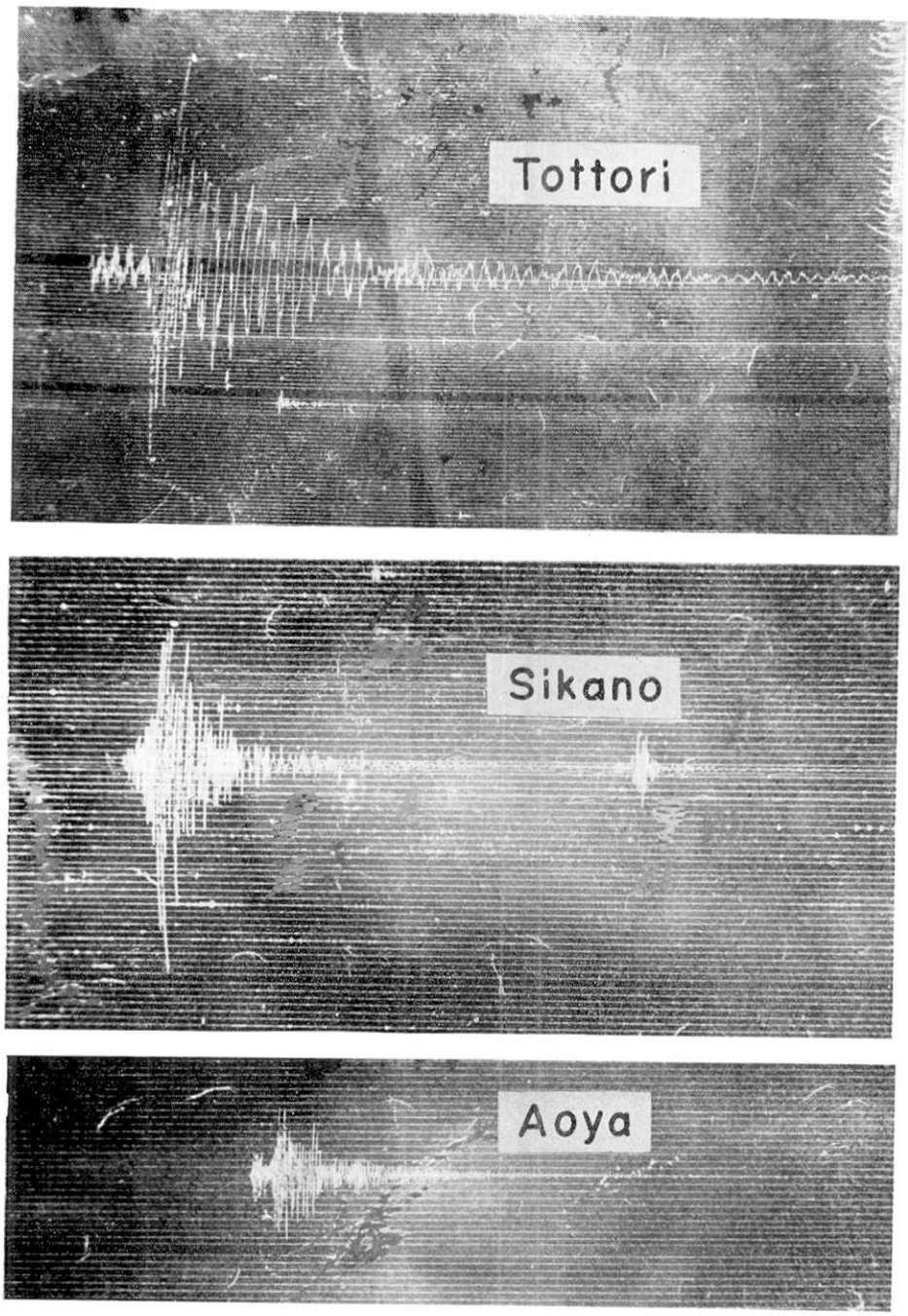

Seismograms of the Tottori aftershocks.

Mr. Akira Jitsukawa who has cooperated with him for the observation of aftershocks, and the author's sincere gratitude is also due to Professor Takahiro Hagiwara for his valuable advices and encouragements.

---

41. 鳥取地震余震観測 (第 2 報)

地震研究所 表 俊 一 郎

昭和 18 年 9 月 10 日夕刻鳥取市及びその附近に大きな災害をもたらした大地震に際しては顕著な地震断層が発現したのでこの断層の追跡，断層面の動きについての精密測定，地電流変化の測定，精密水準測量等興味ある観測が多くの研究者により行はれた．筆者はこの地震の余震の観測を担当し 8 箇所の臨時観測点をもうけて余震観測を行つた．結果の概報は地震直後の彙報に報告せられたけれども，精しい記録の整理は其の後の戦局の激化にあつて延期させられた侭になつていたが今回機会を得て記録の整理を行うことができたのでここにその結果を報告する次第である．震源をきめるにはこの場合も亦専ら *P-S* 時による方法を用いなくてはならなかつた．距離係数 k の値は $k=8.1$ となつた．この値は丹後地震の k の値とほぼ等しく，他の多くの余震観測より得られている値よりは可なり大きい．丹後，鳥取等の余震の k の値が大きいのは山陰地方の地質構造と密接な関係があると考へられる．

鳥取余震の場合には，本震後 18 日目に倉吉附近に震度 IV の可なりの地震が発生し (No. 17 Fig. 8) その後は，いはばこの地震の余震ともいうべき小地震がこの地震の北東の地域に非常に沢山発生するのが見られた．

余震活動域全域にわたつて余震活動の消長がどのような経過をたどつたかを見るために鳥取，鹿野，倉吉の 3 つの観測点をえらび，夫々の観測点で観測された地震の中適当な大きさの地域の中で起つたと考へられる地震について坪井の 式 に従つてそれら 1 つ 1 つの地震の magnitude M をきめそれよりエネルギー E を求めてそれらの M, E 等について若干の考察を行つた．
